Evaluating real-time control of stormwater drainage network and green stormwater infrastructure for enhancing flooding resilience under future rainfall projections

Jiada Li[1] and Steven Burian[2]

[1]Department of Civil and Environmental Engineering, Colorado State University, Fort Collins, CO, USA
[2]Affiliation not available

March 6, 2023

Abstract

Traditional stormwater control measures are designed to handle system loadings induced by fixed-size storm events. However, climate change is predicted to alter the frequency and intensity of flooding events, stimulating the need to explore another more adaptive flooding solution like real-time control (RTC). This study assesses the performance of RTC to mitigate impacts of climate change on urban flooding resilience. A simulated, yet realistic, urban drainage system in Salt Lake City, Utah, USA, shows that RTC improves the flooding resilience by up to 17% under climatic rainfall changes. Compared with green stormwatrer infrastructure (GSI), RTC exhibits a lower resistibility, lower flooding failure level, and higher recovery rate in system performance curves. Results articulate that keeping RTC's performance consistent under 'back-to-back' storms requires a tradeoff between upstream dynamical operation and downstream flooding functionality loss. This research suggests that RTC provides a new path towards smart and resilient stormwater management strategy.

This manuscript is a preprint and has been submitted to the Resources, Conservation and Recycling. Please note that this manuscript is undergoing peer-review, and has not been accepted for publication. Subsequent versions of this manuscript may have slightly different content. If accepted, the final version of this manuscript will be available via the 'Peer-reviewed Publication DOI' link. Please feel free to contact the corresponding author if you have any questions. We appreciate your feedback.

Evaluating real-time control of stormwater drainage network and green stormwater infrastructure for enhancing flooding resilience under future rainfall projections

Jiada Li[1*], Steven J. Burian[2]

[1]Department of Civil and Environmental Engineering, Colorado State University, Fort Collins, CO, 80521 USA

[2]Department of Civil, Construction, and Environmental Engineering, University of Alabama, Tuscaloosa, AL, 35487 USA

[*]Corresponding author, Jiada.Li@colostate.edu

Abstract: Traditional stormwater control measures are designed to handle system loadings induced by fixed-size storm events. However, climate change is predicted to alter the frequency and intensity of flooding events, stimulating the need to explore another more adaptive flooding solution like real-time control (RTC). This study assesses the performance of RTC to mitigate impacts of climate change on urban flooding resilience. A simulated, yet realistic, urban drainage system in Salt Lake City, Utah, USA, shows that RTC improves the flooding resilience by up to 17% under climatic rainfall changes. Compared with green stormwatrer infrastructure (GSI), RTC exhibits a lower resistibility, lower flooding failure level, and higher recovery rate in system performance curves. Results articulate that keeping RTC's performance consistent under 'back-to-back' storms requires a tradeoff between upstream dynamical operation and downstream flooding

functionality loss. This research suggests that RTC provides a new path towards smart and resilient stormwater management strategy.

Keywords: smart city, urban drainage modeling, rainfall nonstationarity, nonlinear dynamical control, continuous flood modeling, long-term resilient stormwater management

1. Introduction

Urban flooding will become more frequent due to climate change increasing the frequency of higher intensity storm event. Historical rainfall changes have contributed approximately 36% of cumulative flooding damages across the U.S. from 1988 to 2017 (Davenport et al., 2021). A 1% increase in historical rainfall intensity increased the urban flooding volume by 1.8% in Salt Lake City, Utah, USA (Li and Burian, 2022). The anticipated continued changes in rainfall patterns challenge the use of historical rainfall and the stationary assumption for design of UDSs (Wright et al., 2019). Given financial constraints and priorities, cities expect UDSs to serve their purpose for 50 years and are now anticipating infrastructure system durability to be 100 years. Considering the present challenges and uncertain future conditions, cities need to consider building adaptability and resilience into their UDSs.

The resilience approach aims to minimize the consequences of system failure through adaptation to changing conditions without permanent loss of functionality (Park et al., 2013). In engineering systems, resilience is defined as the adaptive capacity to resist to, recover from, and adapt to intentional anthropogenic attacks, unpredictable natural events, and human-made disturbances (Holling, 1973). The stormwater engineering field incorporates resilience design complementarily

to risk-based design to minimize flooding duration and magnitude (Jiada Li et al., 2023b; Jiada. Li, 2021). The key benefit of adding resilience design is to mitigate exceptional disturbances, such as rainfall and imperviousness changes, leading to the system functionality loss (Butler et al., 2017). Resilience applied in stormwater engineering can be interpreted as designing a UDS by optimizing resilience profiles composed of resistance, failure, recovery, and adaptation (Ahern, 2011; Ouyang et al., 2012). However, with the use of resilience analysis recently being introduced, questions remain about how rainfall change and imperviousness change will affect the resilience phases of resistance, failure, recovery, and adaptation (Butler et al., 2014).

Urban flooding can be mitigated by upgrading and re-sizing stormwater infrastructure, such as pipes, pump stations, and storage tanks, which convey stormwater runoff into downstream receiving water bodies. Previous studies focused on enhancing resilience through rehabilitating and redesigning UDSs (Mohammadiun et al., 2020), adding system storage components (Mugume et al., 2015), and optimizing the drainage system's structure (Bakhshipour et al., 2021). The locations of structural facilities and the layout of pipelines affect UDS resilience (Zhang et al., 2021). Green stormwater infrastructure (GSI), particularly permeable pavement, bio-retention, and green roofs, are more cost-effective than system rehabilitation when seeking to introduce resilience to climate change and urbanization (Dong et al., 2017; Salerno et al., 2018). GSI, which mimics the natural hydrological process to absorb excess discharge and reduce surface runoff in the form of small-scale distributed practices, is a proven effective solution for small-scale pluvial flooding (Feng et al., 2016; Li et al., 2019b). However, Hou et al. (2020) found that current stormwater gray and green infrastructure are insufficient to ensure the future resilience of UDSs under climate change. Additionally, these passive and static flood controls are designed to meet fixed

performance criteria, but once constructed, they fail to adapt to the exceptional climate changes (Jiada Li, 2021).

Smart stormwater systems with real-time control (RTC) have re-emerged as an adaptive solution to improve infrastructure performance in mitigating urban flooding dynamically. The implementation of RTC contributes to reducing the drainage peak flow (Schmitt et al., 2020; Shishegar et al., 2019), diminishing urban flooding volume (Li, 2020; Mullapudi et al., 2020), controlling combined sewer overflow (Rathnayake and Faisal Anwar, 2019), keeping streams healthy (Xu et al., 2020), and improving water and stormwater quality (Sharior et al., 2019; Troutman et al., 2020). Implementing RTC involves retrofitting (or building with new) UDSs with water level sensors, flow sensors, actuators, and moveable gates to achieve real-time sensing and controlling of system operations (Marchese et al., 2018; Schütze et al., 2004). Sensors provide real-time system states for actuators, which accordingly open or close gates to some extent until the next sensed information changes operations (Li et al., 2023; Li et al., 2020b, 2019a). UDSs can be controlled in real-time to make full use of the available or under-used storage capacity, to retain water in a tank and GSI, or to selectively discharge water before the next storm comes (Lewellyn and Wadzuk, 2017).

The potential to enhance flooding resilience under future rainfall conditions needs further study. Prior studies solely consider assessing resilience changes under artificially designed single rainfall events (Dong et al., 2017; Mugume et al., 2014). Wang et al. (2019) found that measuring resilience based on single storms overestimates the resilience by 18% to 33%, compared with continuous rainfall, in study of changes due to climate change. When simulating RTC under a

single event, the storage volumes are initially empty or partially filled, and once the storm has passed, tanks are slowly drained. However, in back-to-back storm scenarios, where another storm begins before the tanks have been entirely drained, those partially drained tanks might not retain sufficient storage capacity to buffer incoming rainfall-runoff events (Wong and Kerkez, 2018). Assessing RTC performance uses long-term data to inform decisions beyond what a short-term event can provide giving more temporal dynamics and flexibility in control actions, which is crucial to improve stormwater system response to continuous rainfall events (Bowes et al., 2020; Sadler et al., 2020). The leading resilience solution, GSI, presents concerns for long-term effectiveness because it requires more frequent on-site inspection and maintenance than gray and smart infrastructures. GSI requires intensive maintenance and performs inconsistently over long periods, which may trigger early system functionality loss (Brasil et al., 2021; Li et al., 2023a; Li et al., 2021, 2019c).

This study seeks to answer the following question: can RTC outperform GSI in enhancing flooding resilience for future design storms and continuous rainfall for a long-term resilient stormwater management? To that end, this study compares the performance between RTC-equipped and GSI-equipped UDSs located in Salt Lake City, Utah, USA. The primary contribution of this work not only improves the understanding of how smart RTC to tackle the climate-driven urban flooding risks but also address the public concerns of the long-term performance in RTC. This is achieved by assessing resilience based on the performance dynamics in the form of time-dependent performance curves. The novelty of the current study comes from utilizing different stages of performance curves to reflect how stepwise RTC actions enhance resilience in a quantitative and graphical manner.

2. Methodology

2.1. System performance curves

Flooding resilience is estimated by the area between the original system performance curve and the actual performance curve at any time after the occurrence of a storm (Mugume et al., 2015). Fig. 1 shows the time-dependent graph profile of the system performance curve, also called the resilience profile graph or resilience envelope, for a failure-causing rainfall event. The system performance curve consists of the original state from t_o to t_{fs} without flooding, flooding state from t_{fs} to t_r, and adapted state from t_r to t_n without flooding. The flooding phase includes the resistance stage from t_{fs} to t_{mf}, failure stage from t_{mf} to t_{rs}, and recovery stage from t_{rs} to t_r. The black solid horizontal line, P_o represents the original performance level of service. The actual system performance curve is $P_i(t)$, at any time t after the occurrence of the i^{th} storm that leads to system failure. Failure is defined as the occurrence of a flooding event. P_{mf} corresponds to the system's maximum failure level resulting from the considered threat. The flooding magnitude is quantified as the distance from P_o to P_{mf}. The flooding duration corresponds to the period of flooding state, which is equal to the failure duration. The system resistibility or resistance is featured as the falling limb of the performance curve. Before the resistance stage, the resilience envelope is called system robustness. The slope from the maximum system failure level to the original performance level is defined as the recovery rate. After the recovery stage, the resilience graph is regarded as the system reliability. Enhancing resilience can be achieved by reshaping the system performance curve. For example, the dashed blue line in Fig. 1 represents a more resilient UDS with a greater resistibility, lower maximum failure magnitude, and a higher quicker recovery rate than the solid black line.

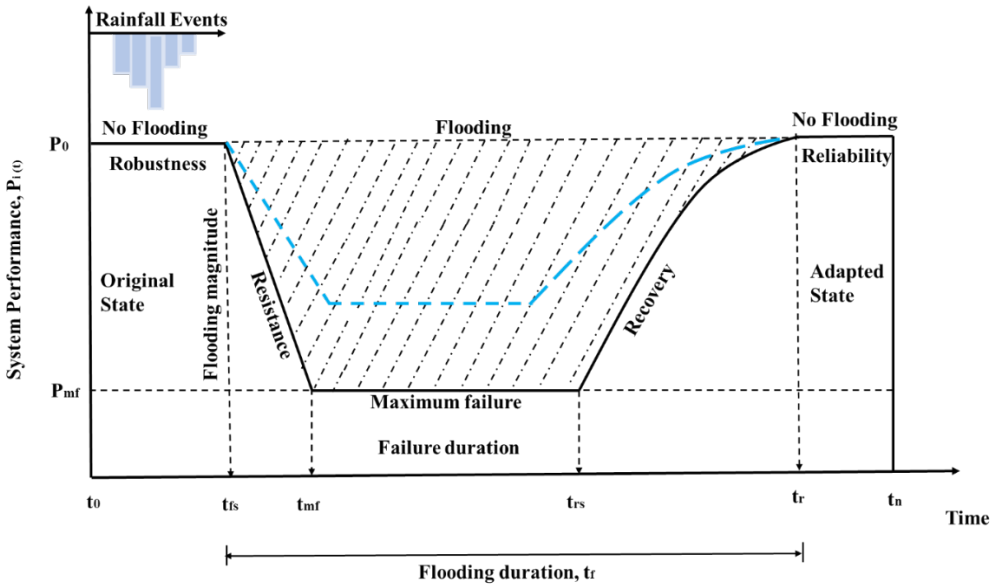

Fig. 1. The system performance curve of an urban drainage system for a failure-causing rainfall event (The t_o is the time of occurrence of storms; The t_{fs} is the flood starting time; The t_{mf} is the starting time of maximum failure; The t_{rs} is the ending time of maximum failure; The t_r is the recovery ending time; The t_f is the flooding duration; The t_n is the total simulation time).

2.2. Flooding resilience computation

The definition of flooding resilience (Res) is a single quantitative index comprised of the magnitude and duration of the system's functional failure during storm events (Casal-Campos et al., 2018; Ouyang et al., 2012). Flooding resilience can be categorized into functional resilience and structural resilience based on the different failure modes (Mugume et al., 2015). This study only focuses on functional flooding resilience under external drivers such as climate change and urban redevelopment. Resilience below refers to functional flooding resilience. The flooding resilience can be quantified by using the concept of flooding severity Sev, which is a function of failure magnitude and failure duration (Hwang et al., 2015; Mugume et al., 2014). Traditionally,

171 the total flooding volume and mean duration of nodal flooding are used to represent the failure
172 magnitude and duration, respectively. The Sev is quantitatively represented as the shaded area
173 (Fig.1) between the original system performance level, P_0 and the actual system performance
174 curve, $P_i(t)$. The shaded rectangular area can be computed by Equation 1, which has been
175 simplified to Equation 2 to approximate the volumetric Sev. The Res is estimated as one minus
176 the computed Sev, shown in Equation 3. However, adopting mean nodal flooding duration to
177 represent the system flooding duration is limited. Firstly, the mean nodal flooding duration is an
178 empirical flooding duration computation. When the nodal flooding duration is not statistically
179 uniform, a mean value might not be representative of all nodes' flooding duration. Secondly, the
180 initially ponded flooding water in the last storm event might be repetitively counted in the next
181 storm events if 'back-to-back' storms continuously occur. The repetitive computation in nodal
182 flooding volume would lead to the over-estimation of flooding duration in continuous modeling.
183 To addresses these issues, this study develops a new resilience computation method for long-term
184 modeling situatios. We used the event flooding duration separated by the inter-event period
185 interval to replace the mean nodal flooding duration of t_F in Equations (4) and (5). This method
186 extends the applicability of flooding resilience for continuous simulations.
187
188 $$Sev = f\left[Sev_p, t_f\right] = \frac{1}{P_0}\int_{t_0}^{t_n}(P_0 - P_i(t))dt \quad (1)$$

189 Where t_f is the failure duration; t_0 is the time of occurrence of the threat; t_n is the total modeling
190 time.

191 $$Sev = \frac{V_{TF}}{V_{T1}} \times \frac{t_r - t_{fs}}{t_n - t_o} = \frac{V_{TF}}{V_{T1}} \times \frac{t_f}{t_n} \quad (2)$$

$$Res = 1 - Sev = 1 - \frac{V_{TF}}{V_{T1}} \times \frac{t_f}{t_n} \quad (3)$$

Where V_{TF} is the total flood volume, V_{T1} is the total inflow into the system, t_f is the mean duration of nodal flooding; t_n is the total simulation time.

$$Sev = \frac{V_{TF}}{V_{T1}} \times \frac{t_r - t_{fs}}{t_n - t_o} = \frac{V_{TF}}{V_{T1}} \times \frac{t_F}{t_n} \quad (4)$$

$$Res = 1 - Sev_i = 1 - \frac{V_{TF}}{V_{T1}} \times \frac{t_F}{t_n} \quad (5)$$

Where V_{TF} is the total flood volume, $V_{T1}$the total inflow into the system, t_F the event flooding duration and t_n the total simulation time.

For a given external disturbance like storm events, Res quantifies the UDS residual functionality as a function of total flooding volume and mean duration of nodal flooding. The Res ranges from 0 to 1. A value of 0 for Res indicates the lowest level of resilience, while 1 is the highest level of resilience. The solid blue line in Fig. 1 represents a more resilient UDS with a small shaded area. Reshaping the resilience graph is to lower maximum failure level and flooding magnitude or to improve resistibility and recovery rate.

3. Case study

3.1 Study drainage catchment overview

The case study drainage catchment is located in the southeastern corner of Salt Lake City, Utah, USA (Fig. 2). Salt Lake City has a semi-arid climate with an average annual precipitation depth of 412 mm, and more than 85% of the rainfall occurring during the spring and summer seasons

(NOAA, 2010). Changes in rainfall intensity from climate change are projected to magnify runoff volume and worsen over-loadings in the local UDSs during rainfall extremes. Consequently, changes in hydrological regimes like the water depths have raised great flooding concerns from local residents (Jiada Li, 2021).

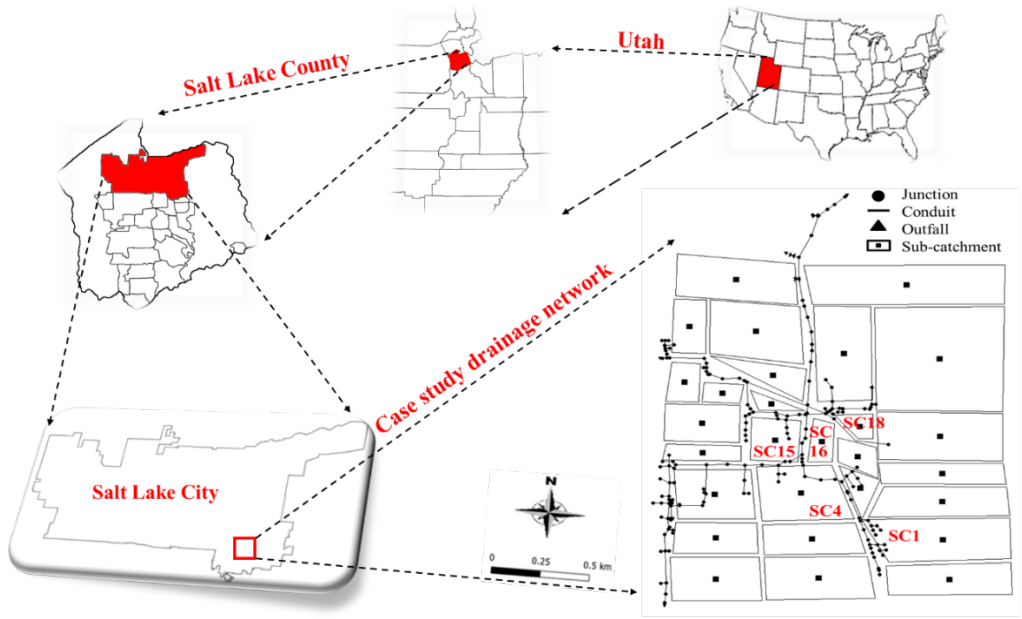

Fig. 2. The study area in the Sugar House area of Salt Lake City, Utah, USA showed alongside the urban drainage network model used in the study.

3.2 Urban drainage model

For this study, we use a drainage system model built using the U.S. Environmental Protection Agency Storm Water Management Model (SWMM) Version 5.1 (Rossman 2015). The model includes 28 sub-catchments, 184 conduits, and 181 junctions, and one rain gauge (Fig. 2). The details of the model development, validation, and parameter settings can be found in previous work (Li and Burian, 2022).

3.2.1 Simulating the effect of adaptation strategies on UDS performance

In this study, two adaptation strategies, RTC of distributed storage tanks and GSI, are implemented to improve resilience.The GSI adaptation strategy used in this study consists of three bio-retention cells and two permeable pavements distributed in the drainage sub-catchments (Fig. 1: bio-retentions in sub-catchments SC15 and 16, permeable pavement in sub-catchments SC1, 4, and 18) of the SWMM model. Bioretention cells and permeable pavement are selected because of the installation accessibility, construction and maintenance budgets, usage of existing facilities, and their performance in a semi-arid environment. These GSI practices are designed to capture the 80th percentile rainfall event, which is the local standard (12.7 mm rainfall depth) (Department of Environmental Quality, 2018), by increasing in SWMM the number GSI units in a sub-cathcment until the stormwater is completely retained. Converting 15% of the impervious area to bio-retention units and 10% to permeable pavement is able to fully retain the stormwater in the study area (SLCDPU, 2018). In the SWMM model, the percent imperviousness of each sub-catchment is accordingly changed to account for the impacts of GSI implementation. For each sub-catchment, 50% of the impervious area is routed to its corresponding bio-retention units, and the other 50% routed to its permeable pavement. The SWMM parameters used in modeling the bio-retention and pervious pavement are listed in Table 1.

Table 1. SWMM model parameter settings for simulating bio-retention cells and permeable pavement (data sources for designing GSIs are referred to previous GSI studies in Salt Lake City (Burian et al., 2009; Feng et al., 2016; Tavakol-Davani et al., 2016, 2019))

Attributes	Parameters	Bio-retention Cells	Permeable Pavement
Surface	Berm height (m)	0.15	0.025
	Vegetation volume fraction	0.45	0.1
	Surface roughness	0.1	0.02
	Surface Slope (%)	1	2
	Thickness (m)	0.075	0
	Porosity	0.7	0.7
	Field capacity	0.16	0.16

Soil	Wilting point	0.1	0.1
	Conductivity (mm/hr)	75	75
	Conductivity slope (%)	30	30
	Suction head (m)	0.5	0.5
Storage	Thickness (m)	0.15	0.3
	Voids ratio	0.25	0.75
	Seepage rate (mm/hr)	18	5
	Clogging factor	0	0
Drainage	Flow coefficient (mm/hr)	0	0
	Flow exponent	0.5	0.5
	Offset height (m)	0.05	0
Pavement	Thickness (m)	None	0.2
	Void Ratio	None	0.15
	Imperviousness	None	0
	Permeability (m/hr)	None	2.54
	Clogging Factor	None	0

RTC adaptation strategy is developed to control three hypothetical orifice gates and three corresponding storage tanks with sizes of 4000, 5000, and 5000 m^3 (Li et al., 2021). The storage volume is designed to meet the capacity to accommodate the total stormwater runoff volume from the upstream contributing sub-catchments and to prevent the tanks' outflow from exceeding the predevelopment system peak flow under the same rainfall event of design GSI. The RTC strategy automatically adjusts the gate opening to control the tank storage volume and outflow. Actions in gates (% openings of gates) are computed by the nonlinear control Equation (4).

$$GO_i = min\left(1, \frac{D_i * R_i}{A * \sqrt[2]{2 * g * Q_i}}\right) \times 100\% \quad (4)$$

Where GO_i is the gate percentage opening at the i^{th} time step; D_i is the tank water depth at the i^{th} time step; R_i is the rainfall intensity at the i^{th} time step; Q_i is the tank outflow at the i^{th} time step; A is the maximum opening area of the gate, and this study assumes the maximum area to be 1 m^2; g is the acceleration of gravity (9.8 m^2/s); min is to select the minimum value between the actual opening output and 1 as the final gate opening, which avoids the gate opening over 100%.

In the nonlinear control equation, including rainfall forecasts as control inputs allows the RTC system to compute coordinated gate actions in advance and prepare available storage volumes for incoming storm events. Meanwhile, the consideration of tank water level and outflow is advantageous to prevent local overflow and downstream flooding issues. Detailed explanations about the development of control rules used in the RTC strategy can be found in Li et al. (2020a) and Li et al. (2021). All adaptation strategies are simulated by using PySWMM, which is a Python language software package for the creation, manipulation, and study of the structure, dynamics, and function of SWMM models throughout stepwise rainfall-runoff simulations (McDonnell et al., 2020).

3.2.2 Future scenarios

Future (2035-2049) daily precipitation datasets from Coupled Model Intercomparison Project Phase 5 (CMIP5) were acquired for the Global Circulation Model (CCSM) 4.1. The CCSM 4.1 was chosen due to the favorable performance in reproducing historical climate for the study area and the wide connection between climatic variability and mean monthly precipitation (Smith et al., 2015). Climate scenarios proposed by the Intergovernmental Panel on Climate Change (IPCC) were Representative Concentration Pathways (RCPs), which reflect the radiative forcing level of climate systems (O'Neill et al. 2016). We selected RCP 4.5 and 8.5 since they cover the range of greenhouse gas emissions from low to high levels. RCP 4.5 represents a moderate scenario that assumes future trends throughout the 21st century will follow the historical patterns, while RCP 8.5 is the worst greenhouse gas emission scenario. The future daily precipitations were downscaled by using the combined change factor method due to its simplicity, efficiency, and acceptable accuracy (Hansen et al., 2017). The downscaled data assumes changes from the historical to the

290 projection period, so we conducted bias-correction with the linear scaling method implemented in
291 the CMhyd tool (Teutschbein and Seibert, 2012). We further disaggregated daily precipitations
292 into hourly resolution by using NetSTORM (Heineman, 2004). This study focused on the warm
293 season months in Salt Lake City (May to September), so the October to April period was not
294 considered in the simulation.
295
296 For the design storm part of the study, hourly rainfall projections were analyzed to generate the
297 future Intensity-Duration-Frequency (IDF) curves using the same approach as the NOAA
298 (National Oceanic and Atmospheric Administration) Atlas 14 for design rainfall events (United
299 States Department of Agriculture, 2009). Fig. 3a shows the future rainfall intensities corresponding
300 to durations of 1-, 3-, 6-, 12-, 24-, and 48-hour and return periods of 1-, 2-, 10-, 25-, 50-, and 100-
301 year for the RCP 4.5 and 8.5 climate scenarios, respectively. These future IDF curves show
302 consistent results to previous studies quantifying climate change impacts on rainfall extremes in
303 Western U.S. cities, like Tucson, Arizona (Tousi et al., 2021). Because of their general relevance
304 for stormwater management, the present study only considers the 3-hour duration and 2-, 10-, 100-
305 year average recurrence interval future rainfalls, which are assigned the Farmer-Fletcher rainfall
306 time distribution developed for the region (Fig. 3b) (Humphrey, 2009). All future rainfalls peak at
307 1:15, and have rainfall intensity with an average of 13% (RCP 4.5) and 25% (RCP 8.5) higher than
308 the historical estimates of NOAA Atlas 14 point precipitation frequency. Fig. 3c shows the 2049
309 continuous rainfalls for RCP 4.5 and 8.5 scenarios. RCP 4.5 includes 7 rainfall events, while RCP
310 8.5 has 8 events highlighted in purple dashed squares. These rainfall events are selected since they
311 cover short- to long-duration and low- to high-intensity events, and these events have an average
312 depths of 21 mm and 20 mm for RCP 4.5 and 8.5 scenarios, respectively; these rainfall depths are

close to the average rainfall depth of 2-year and 3-hour rainfall event in the study area.

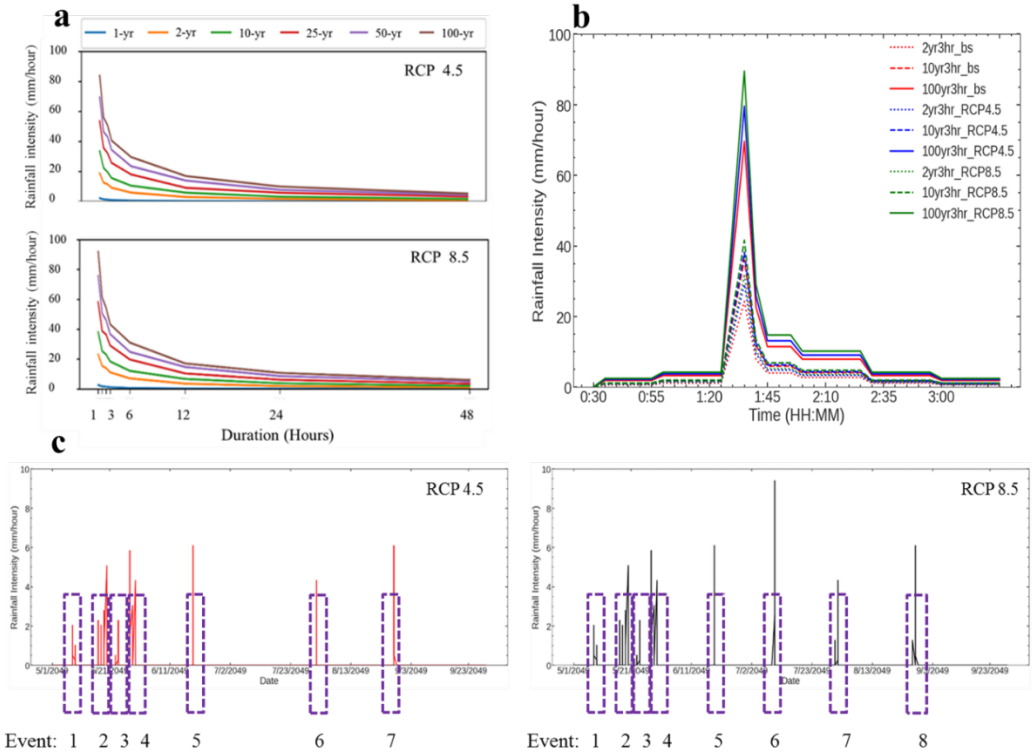

Fig. 3. A graphic combination of a) future IDF curves, b) future design rainfalls of 3-hour duration and 2-, 10-, and 100-year return periods, and c): 2049 future continuous rainfalls under RCP4.5 and 8.5 climate scenarios.

We compared the RTC and GSI performance for enhancing flooding resilience under the following simulation scenarios:

1) Future Baseline (BS): SWMM model driven by future design storms and continuous rainfall of RCP 4.5 and 8.5 without GSI and RTC
2) GSI: Same as BS but with GSI retrofits;
3) RTC: Same as BS but with control retrofits.

Continuous modeling outcomes, including time-series gate opening, tank outflow, system inflow, and flooding volume and duration, were collected at each timestep to quantify the system performance curve and resilience changes and investigate the system responses after adaptation.

4. Results

4.1 Performance comparison under future design storms

System performance curves are significantly reshaped by GSI and RTC adaptation strategies. Fig. 4 shows that GSI and RTC elevate the UDS's maximum failure (worst performance) level and accelerate the system recovery rate, compared with the baseline scenario. GSI and RTC have smaller flooding severity volumetric areas than the baseline system, indicating GSI and RTC can improve the UDS performance on RCP 4.5 climate scenario. Particularly, the top subplot of Fig. 4 shows that GSI enables the system to have a higher maximum failure level of 0.97 than the RTC (0.96) for the 2-year 3-hour event. As storm size increases to 10-year, the maximum failure level of GSI drops slightly below the RTC, but it is still higher than the baseline in the middle subplot of Fig. 4. As the storm return period increases to 100-year, GSI shows limited influences on subsiding the flooding severity volumetric area in comparison to the baseline system (bottom subplot of Fig. 4).

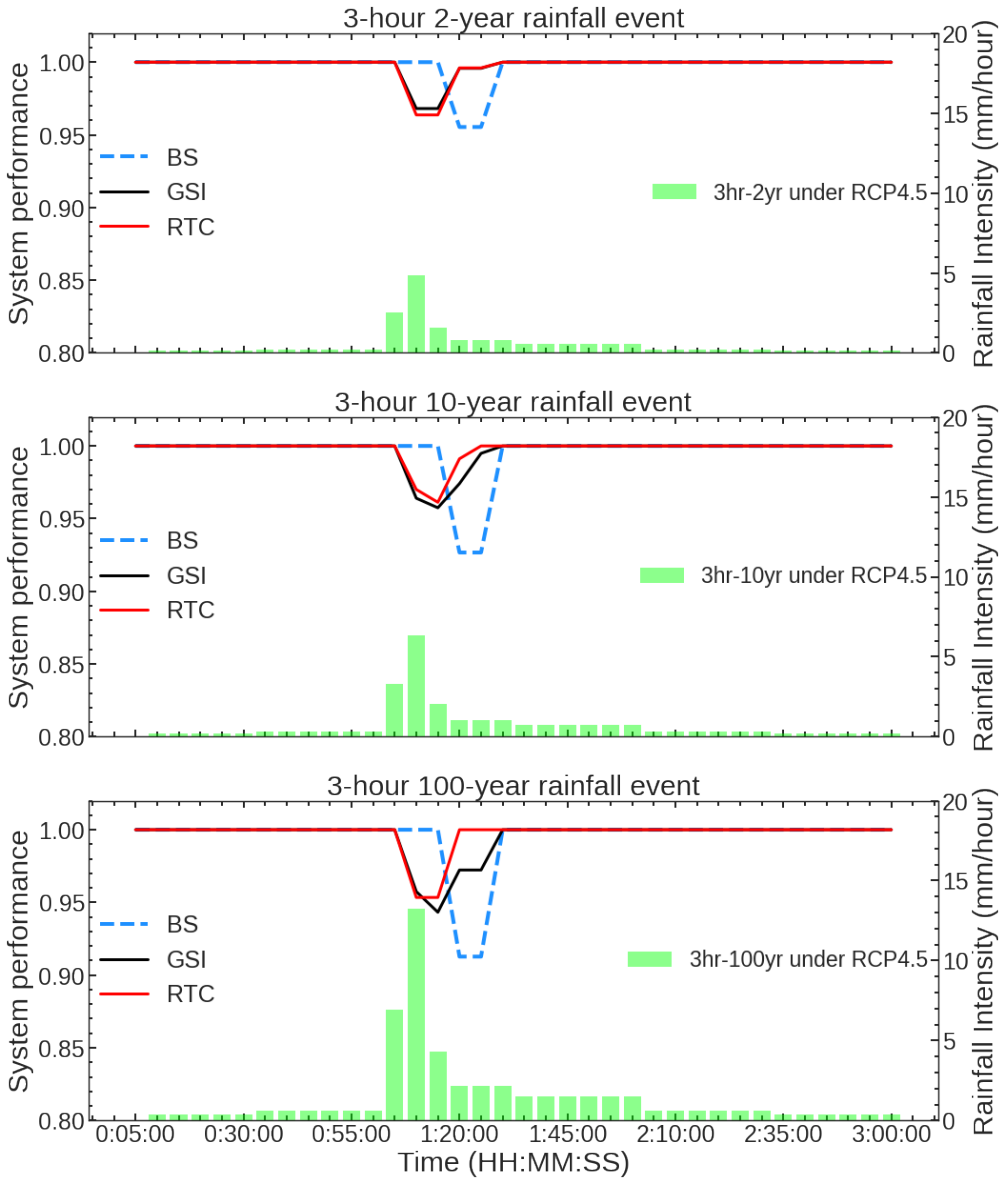

342

343 **Fig. 4.** System performance curves for the 3-hour and 2-year, 10-year, and 100-year future rainfall events under RCP

344 4.5 climate scenario.

345

346 RTC retains the adaptive capacity as rainfall intensity increases. Fig. 5 shows that RTC has few

347 changes in failure level and flooding severity volumetric area from small to large rainfall events.

348 This finding illustrates that RTC is able to protect the system's functionality by addressing the

349 impacts across a range of design storms. Without adaptations, the maximum failure level

significantly declines from 0.9 to about 0.6, and the flooding severity volumetric area doubles from small (top subplot of Fig. 5) to large (middle subplot of Fig. 5) storms. With GSI retrofits, the UDS has the maximum failure level decreasing from 0.95 to 0.78 from 2-year to 100-year rainfall events. Even worse, GSI lessens the system functionality in the RCP 8.5 scenario. The middle subplot of Fig. 5 shows that the maximum failure level of GSI surprisingly falls below the baseline system, and induces a significantly larger severity volumetric area than RTC during the 100-year 3-hour storm event (bottom subplot of Fig. 5). GSI is designed like the passive gray stormwater infrastructure to meet fixed stormwater criteria, but increased rainfall volume and intensity can surpass these design standards leading to increases in flooding. In contrast, RTC adjusts the system operations to cope with the changes in rainfall and runoff volume.

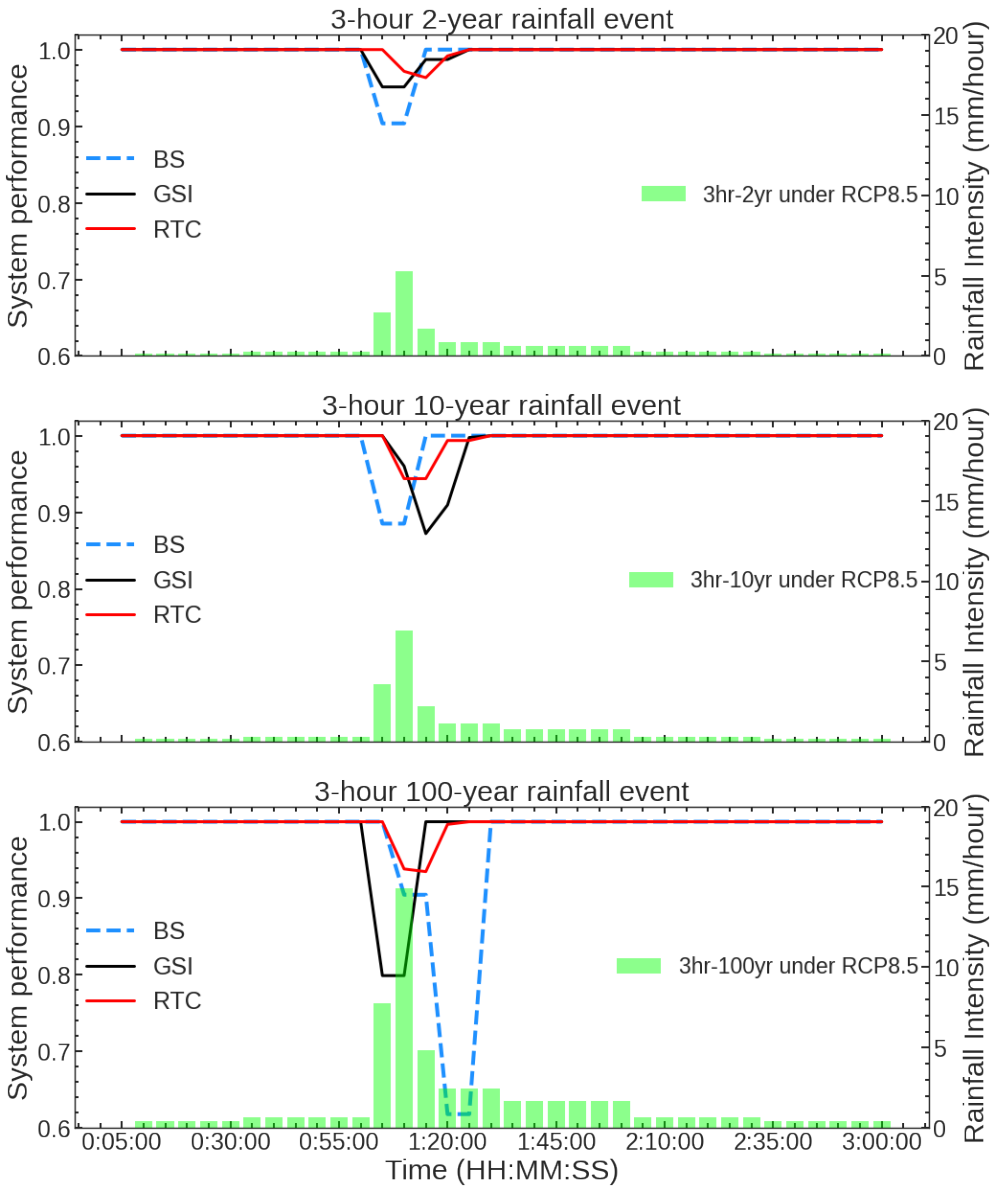

361

362 **Fig. 5.** System performance curves for the 3-hour and 2-year, 10-year, and 100-year future rainfall events under RCP

363 8.5 climate scenario. Please note the left y-axis has different intervals and ranges for each subplot.

364

365 Although the system is overwhelmed in the 100-year storm event, RTC makes full use of the

366 available storage to retain the additional flooding volume. This operation can be done by

367 expanding gate opening magnitude and extending the duration of 100% full opening. In general,

368 RTC opens gates a larger percentage under 100-year event than under the 2- or 10-year event

loadings (Fig. 6). RTC senses the runoff peaking time in advance so that outflow can be timely discharged to prepare sufficient storage for incoming events. For instance, Fig. 6 shows that RTC continues opening the gate to 100% for 20 minutes (1:10-1:30) at the 100-year rainfall peaking time, and then gradually closes the gate to about 20% from 1:30 to 3:00. During this period, the storage tanks release the biggest amount of outflow to prepare the maximum storage volume. The dynamic operation is found to be the key reason why RTC is advantageous to the GSI's static performance when dealing with future rainfall extremes.

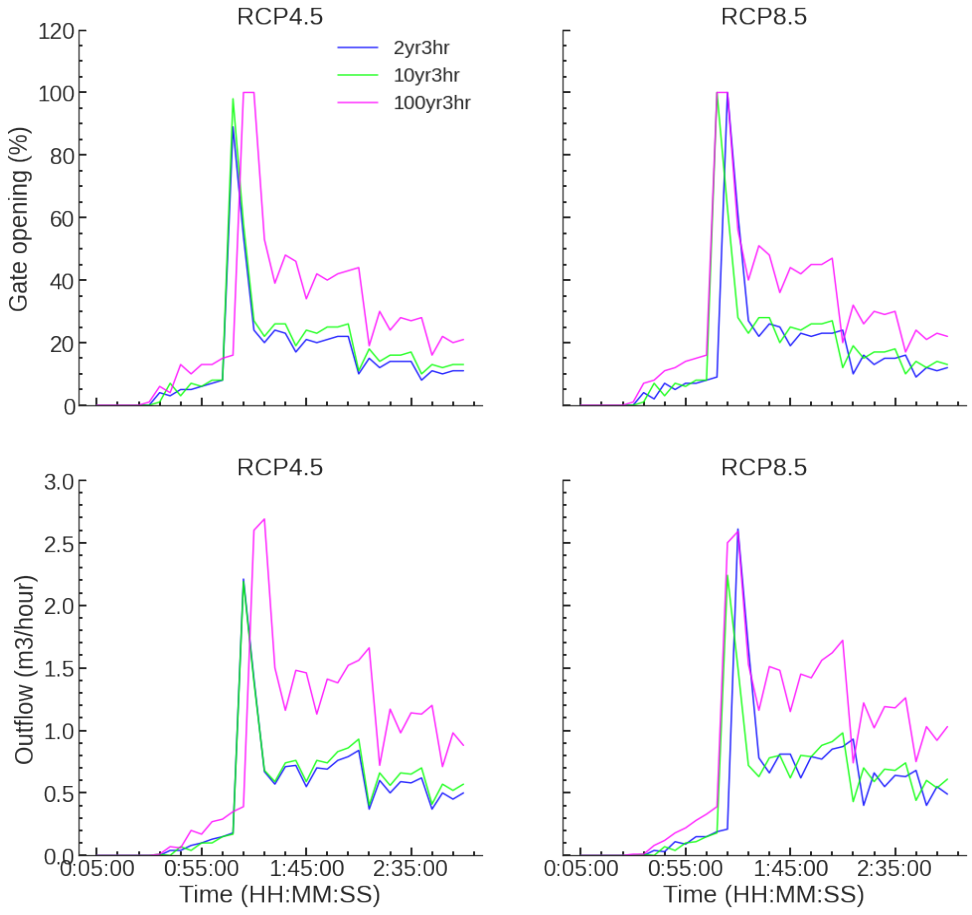

Fig. 6. RTC dynamically opens the gate to release outflow for preparing sufficient storage volume for storm events under RCP 4.5 and RCP 8.5 climate scenarios.

RTC shows greater performance for achieving higher resilience for rainfall events beyond the 10-year design storms. GSI amplifies the flooding resilience up to 5% and 13% for RCP 4.5 and RCP 8.5 100-year storms in Fig. 7. RTC improves the resilience up to about 6% and 17% at the 100-year event for RCP 4.5 and RCP 8.5, respectively.

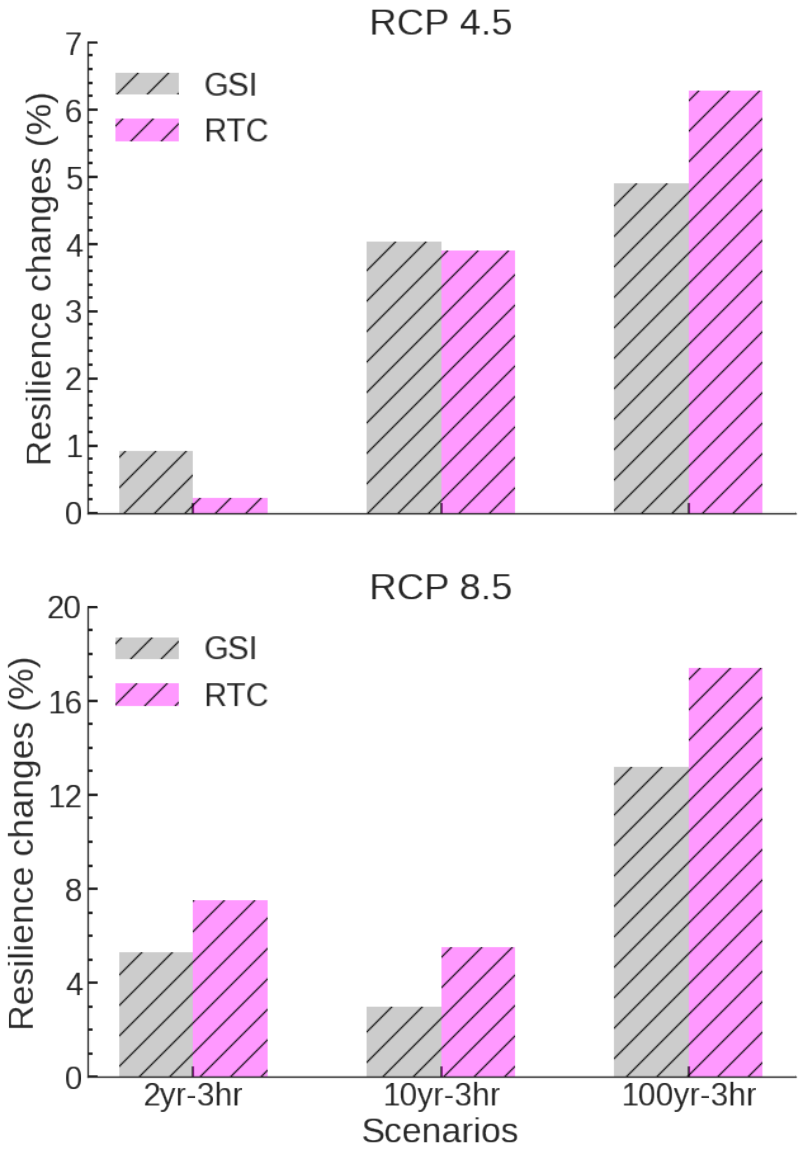

Fig. 7. Resilience relative changes from GSI or RTC adaptation strategy to the baseline model under future artificially-designed rainfalls of RCP 4.5 and RCP 8.5 climate scenarios.

390 **4.2. Performance comparison under future continuous rainfalls**

391 RTC consistently outperforms GSI during the long-term continuous simulations. During rainfall
392 peaks, the RTC and GSI adaptations significantly improve upon the baseline system performance
393 (blue curves in Fig. 8). Events 1-4 (05/01/2049 to 06/01/2049) show larger differences in flooding
394 severity volumetric areas between the baseline curve and adaptation curve than other storms after
395 June 2049. This can be attributed to the fact that events 1-4 generally have longer storm durations
396 than events 5-8, shown in Table 2. In RCP 4.5 climate scenario, RTC has higher performance
397 curves (red curves) than GSI (black curves) at any time the occurrence of storm events in Fig.8.
398 Still, such a finding is not applicable to the rainfall events of RCP 8.5 climate scenario. This
399 discovery can be explained by Fig. 9, which shows that GSI has relatively higher performance than
400 RTC at the system resistance stage. Especially under 'back-to-back' events 5-8 (medium or high
401 rainfall intensity) of RCP 8.5, GSI has slower falling limbs of performance curves than RTC (Fig.
402 9), indicating that GSI retrofit is more important to improve system resistibility than RTC.
403

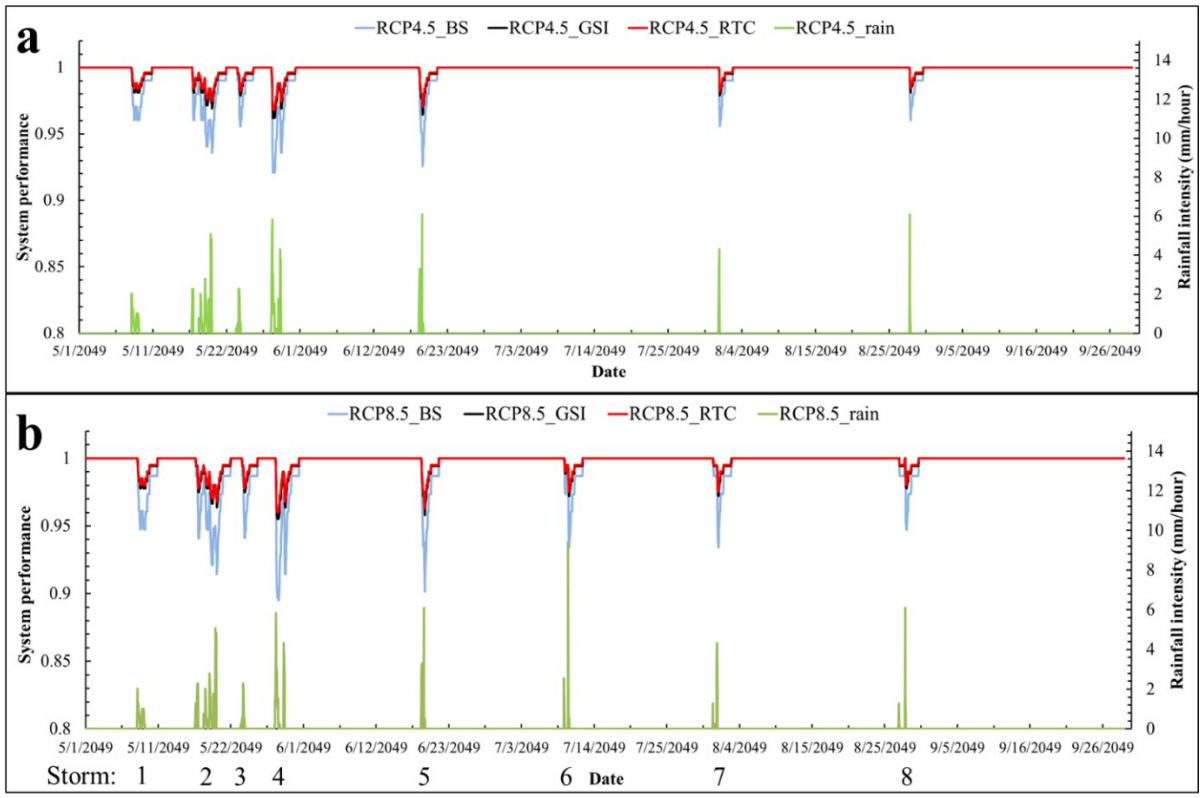

404

405 **Fig. 8.** System performance curves for 2049 continuous future rainfalls under a) RCP 4.5 and b) RCP 8.5 climate
406 scenarios.

407

408 However, improving system resistibility does not necessarily mean enhancing system resilience.
409 RTC has lower failure levels and faster recovery rates than GSI (recovery stage of Fig. 9), resulting
410 in a higher resilience than GSI in future storms ranging from the short to long duration and low to
411 high intensity.The advantage of the RTC is to improve system maximum failure level and recovery
412 rate, while GSI is superior to improve the system resistance capacity. These adaptation benefits,
413 consequently, promote system resilience under future climatic impacts.

414

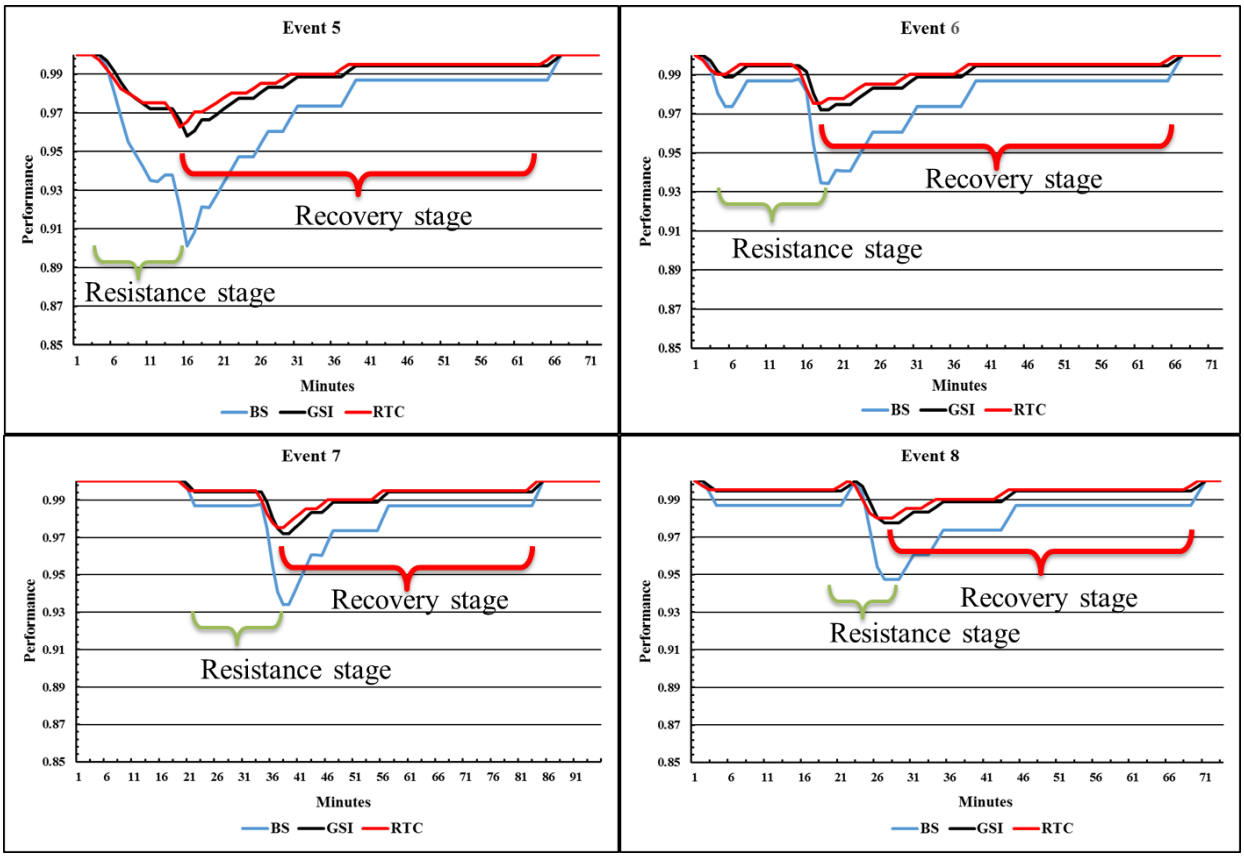

Fig. 9. System performance curves under continuous storm events of RCP 8.5 climate scenario. During the resistance stage, GSI (black curves) has higher performances than RTC (red curves), but this phenomenon reverses at the recovery stage.

5. Discussion

The present research finds that RTC has inconsistent performance during continuous 'back-to-back' storms due to the system functionality loss in the resistance stage of performance curves. During the 'back-to-back' storms, RTC only opens gates from 0% up to 25% when runoff peaks, and ends up fully closing the gate when rainfall recesses. In this way, water is still retained in the storage tank when the subsequent storm comes. This operation avoids releasing overloaded water to the downstream catchments to cause downstream flooding. Also, it ensures a certain amount of

stormwater discharge and prepares sufficient storage volume for the incoming storms. However, the deposited water diminishes the initial storage capacity of the UDS system and loses the system's functionality. The RTC's performance curve drops earlier than GSI in events of RCP 8.5 climate scenario (Fig. 9), which is the reason why GSI has resistibility exceeding RTC during the initial flooding stage. Such a case does not exist in designed storm events. During a single storm event, RTC gradually opens the gate to 100% when rainfall peaks, and ends up partially closing the gate when rainfall goes away (Fig. 6). In this case, no water is ponded in the storage tank when the next storm comes. As such, the RTC remains stable in performance without resistance functionality loss for design storms.

The functionality loss in RTC can be offset by the following smaller failure level and quicker recovery speed than GSI. Referring to the recovery stages of performance curves in Fig. 9, we discover that RTC performance stops declining at a higher bottom point and then reverses back to original states with a higher performance than GSI. These changes reflect the high level of adaptivity and flexibility of RTC due to dynamic operations to cope with changing conditions. The increased adaptivity and flexibility, as two resilience attributes, directly enhance the system's resilience. Fig. 10 shows that RTC has higher resilience than GSI, but the resilience differences become smaller from RCP4.5 to RCP8.5 scenarios. Future work will focus on how to maintain consistency in RTC performance during long-term simulations with various flooding events of different volumes, durations, and intensities. RTC retains water in the system after prior storms, which reduces the initial storage capacity available for the next storms, but prevents the floods from occurring in downstream hotspots (Li et al., 2020b). In contrast, GSI completely infiltrates and discharges water into drainage inlets during storm events, which promotes the initial storage

capacity and system resistibility for the next rainfall events. These findings coincide with those reported in previous literature (Dong et al., 2017; Tavakol-Davani et al., 2016), but GSI still fails to handle large (100-year) floods in our case.

The 100% gate opening for mitigating the runoff peaks is acceptable since the RTC operation has the potential to reduce functionality loss and enhance flooding resilience. However, fully opening the gate would cause a higher outflow to trigger downstream flooding when the next storm arrives before discharge ends. Simply releasing upstream storage tanks' outflow into downstream catchments cannot boost the flooding resilience, which agrees with the catchment flooding resilience study (Wang et al., 2019). The resilience improvement under 'back-to-back' storms needs a system view. Thus, building the tradeoff between the gates' dynamical operation and system's functionality loss is crucial to keep consistent control performance in the long-term period. Control operation process increases system storage capacity but may lead to system functionality loss due to the occurrence of downstream flooding. This information is of great importance for guiding stormwater engineers, who have expertise in stormwater infrastructure design and can gain from understanding controls and how to implement RTC to adapt to future rainfall changes.

6. Conclusions

In the age of climate adaptation, the present study contributes to resilience advancements in Urban Drainage Systems (UDSs) by smart and green stormwater infrastructure retrofits for long-term resilient stormwater management. This research work compares the performance of real-time control (RTC) and green stormwater infrastructure (GSI) to mitigate the impacts of climate change

on urban flooding in Salt Lake City, Utah, USA. The comparison of resilience changes highlights that RTC can perform better than GSI as a crucial component of long-term resilient stormwater management. This study covers the flooding resilience assessment under various disturbances induced by future single and continuous rainfalls scenarios, which is helpful to improve the understanding of the temporal dynamics in system performance and functionality loss. Under a single storm, we summarized that both GSI and RTC are effective adaptation strategies by improving resilience by up to 13% and 17%, respectively, by 2049. As the storm size increases over the 10-year return period, GSI is less capable of enhancing system performance and resilience than RTC. Under future 'back-to-back' storms, we concluded that the performance curves of GSI have a stronger resistance capability while RTC has a faster recovery future from RCP (Representative Concentration Pathway) 4.5 to 8.5 climate scenarios. Our research represents the first step to explore how to build a long-term climate-adaptation strategy tailored for existing UDSs under various rainfall scenarios for smart stormwater community.

Data Availability Statement

Some or all data, models, or code that support the findings of this study are available from the corresponding author upon reasonable request (SWMM model, part of datasets, and codes for modeling RTC).

Acknowledgments

493 This research was funded by the project (835866-01) of Prediction of Nonlinear Climate Variations
494 Impacts on Eutrophication and Ecosystem Processes and Evaluation of Adaptation Measures in
495 Urban and Urbanizing Watersheds from the U.S. Environmental Protection Agency.

496

497 # References

498 Ahern, J., 2011. From fail-safe to safe-to-fail: Sustainability and resilience in the new urban world. Landsc. Urban
499 Plan. 100, 341–343. https://doi.org/10.1016/j.landurbplan.2011.02.021
500 Bakhshipour, A.E., Dittmer, U., Haghighi, A., Nowak, W., 2021. Toward Sustainable Urban Drainage Infrastructure
501 Planning: A Combined Multiobjective Optimization and Multicriteria Decision-Making Platform. J. Water
502 Resour. Plan. Manag. 147, 04021049. https://doi.org/10.1061/(asce)wr.1943-5452.0001389
503 Bowes, B.D., Tavakoli, A., Wang, C., Heydarian, A., Behl, M., Beling, P.A., Goodall, J.L., 2020. Flood mitigation in
504 coastal urban catchments using real-time stormwater infrastructure control and reinforcement learning. J.
505 Hydroinformatics 23, 529–547. https://doi.org/10.2166/hydro.2020.080
506 Brasil, J., Marina, M., Thalita, O., Marcus, J., Tassiana, O., Eduardo, M., 2021. Nature-Based Solutions and Real-
507 Time Control Challenges and Opportunities. Water 13, 651. https://doi.org/10.3390/w13050651
508 Burian, S., Dietz, M., Pomeroy, C., Görges, B., Flower, W., 2009. Low impact development in Utah: Progress,
509 constraints, and future outlook, Low Impact Development for Urban Ecosystem and Habitat Protection.
510 https://doi.org/10.1061/41009(333)75
511 Butler, D., Farmani, R., Fu, G., Ward, S., Diao, K., Astaraie-Imani, M., 2014. A new approach to urban water
512 management: Safe and sure. Procedia Eng. 89, 347–354. https://doi.org/10.1016/j.proeng.2014.11.198
513 Butler, D., Ward, S., Sweetapple, C., Astaraie-Imani, M., Diao, K., Farmani, R., Fu, G., 2017. Reliable, resilient and
514 sustainable water management: the Safe & SuRe approach. Glob. Challenges 1, 63–77.
515 https://doi.org/10.1002/gch2.1010
516 Casal-Campos, A., Sadr, S.M.K., Fu, G., Butler, D., 2018. Reliable, Resilient and Sustainable Urban Drainage
517 Systems: An Analysis of Robustness under Deep Uncertainty. Environ. Sci. Technol. 52, 9008–9021.
518 https://doi.org/10.1021/acs.est.8b01193

519 Davenport, F. V, Burke, M., Diffenbaugh, N.S., 2021. Contribution of historical precipitation change to US flood
520 damages. Proc. Natl. Acad. Sci. U. S. A. 118, 1–7. https://doi.org/10.1073/pnas.2017524118
521 Department of Environmental Quality, U., 2018. A Guide to Low Impact Development within Utah [WWW
522 Document]. URL https://documents.deq.utah.gov/water-quality/stormwater/updes/DWQ-2019-000161.pdf
523 (accessed 1.9.21).
524 Dong, X., Guo, H., Zeng, S., 2017. Enhancing future resilience in urban drainage system: Green versus grey
525 infrastructure. Water Res. 124, 280–289. https://doi.org/10.1016/j.watres.2017.07.038
526 Feng, Y., Burian, S., Pomeroy, C., 2016. Potential of green infrastructure to restore predevelopment water budget of
527 a semi-arid urban catchment. J. Hydrol. 542, 744–755. https://doi.org/10.1016/j.jhydrol.2016.09.044
528 Hansen, C.H., Goharian, E., Burian, S., 2017. Downscaling precipitation for local-scale hydrologic modeling
529 applications: Comparison of traditional and combined change factor methodologies. J. Hydrol. Eng. 22.
530 https://doi.org/10.1061/(ASCE)HE.1943-5584.0001555
531 Heineman, M.C., 2004. NetSTORM - A computer program for rainfall-runoff simulation and precipitation analysis,
532 in: Proceedings of the 2004 World Water and Environmetal Resources Congress: Critical Transitions in Water
533 and Environmetal Resources Management. pp. 3455–3468. https://doi.org/10.1061/40737(2004)395
534 Holling, C.S., 1973. Resilience and Stability. Annu. Rev. Ecol. Syst. 4, 1–23.
535 Honardoust, D.R., 2020. Assessment of Predictive Real-Time Control Retrofits on Stormwater Basin Performance in
536 an Urban Watershed. Virginia Tech.
537 Hou, X., Guo, H., Wang, F., Li, M., Xue, X., Liu, X., Zeng, S., 2020. Is the sponge city construction sufficiently
538 adaptable for the future stormwater management under climate change? J. Hydrol. 588, 125055.
539 https://doi.org/10.1016/j.jhydrol.2020.125055
540 Humphrey, J.H., 2009. CITY OF ST. GEORGE stormwater design [WWW Document]. Brown Colloins Assoc. Inc.
541 URL
542 https://www.sgcity.org/pdf/transportationandengineering/engineering/drainageguidelinesandhydrology/draina
543 geguidelinesandhydology.pdf (accessed 2.11.20).
544 Hwang, H., Lansey, K., Quintanar, D.R., 2015. Resilience-based failure mode effects and criticality analysis for
545 regional water supply system. J. Hydroinformatics 17, 193–210. https://doi.org/10.2166/hydro.2014.111
546 Lewellyn, C., Wadzuk, B., 2017. Evaluating green infrastructure performance using real-time control from a risk

perspective, in: Water Environment Federation Technical Exhibition and Conference 2017, WEFTEC 2017. pp. 4726–4733. https://doi.org/10.2175/193864717822156668

Li, Jiada., 2021. Smart Stormwater Real-Time Control to Enhance Urban Flooding Resilience Against Nonstationarity in Rainfall and Urban Land Cover. The University of Utah.

Li, Jiada, 2021. Exploring the Potential of Utilizing Unsupervised Machine Learning for Urban Drainage Sensor Placement under Future Rainfall Uncertainty. J. Environ. Manage. 296, 113191.

Li, J., 2020. A data-driven improved fuzzy logic control optimization-simulation tool for reducing flooding volume at downstream urban drainage systems. Sci. Total Environ. 732, 138931. https://doi.org/10.1016/j.scitotenv.2020.138931

Li, J., Bao, S., Burian, S., 2019a. Real-time data assimilation potential to connect micro-smart water test bed and hydraulic model. H2Open J. 2, 71–82. https://doi.org/10.2166/h2oj.2019.006

Li, J., Burian, S., Oroza, C., 2021. Exploring Cost-effective Implementation of Real-time Control to Enhance Flooding Resilience against Future Rainfall and Land Cover Changes. J. Hydrol. Under Review.

Li, Jiada., Burian, S., Oroza, C., Johnson, R., 2023. Modeling Operations in System-level Real-time Control for Urban Flooding Reduction and Water Quality Improvement – An Open-source Benchmarked Case. Sensors (Switzerland) Under review.

Li, Jiada, Burian, S., Oroza, C., Johnson, R., 2023a. Exploring Cost-effective Implementation of Real-time Control to Enhance Flooding Resilience against Future Rainfall and Land Cover Changes. Sci. Total Environ. under revi.

Li, Jiada, Burian, S., Strong, C., 2023b. Assessing Impacts of Future Land Cover and Rainfall Change on Urban Flooding Using An Event-based Resilience Index. J. Clean. Prod. Under Revi.

Li, J., Burian, S.J., 2022. Effects of Nonstationarity in Urban Land Cover and Rainfall on Historical Flooding Intensity in a Semiarid Catchment. J. Sustain. Water Built Environ. https://doi.org/10.1061/jswbay.0000978

Li, J., Oroza, C., Burian, S., 2020a. Evaluating Real-time Control Performance on System-level Urban Flooding Reduction and Water Quality Improvement. EarthArXiv https://doi.org/10.31223/osf.io/y43j7.

Li, J., Tao, T., Kreidler, M., Burian, S., Yan, H., 2019b. Construction Cost-Based Effectiveness Analysis of Green and Grey Infrastructure in Controlling Flood Inundation: A Case Study. J. Water Manag. Model. 27, C466. https://doi.org/10.14796/jwmm.c466

Li, J., Yang, X., Sitzenfrei, R., 2020b. Rethinking the framework of smart water system: A review. Water (Switzerland)

12, 412. https://doi.org/10.3390/w12020412

Marchese, D., Johnson, J., Akers, N., Huffman, M., Hlas, V., 2018. Quantitative comparison of active and passive stormwater infrastructure: Case study in Beckley, West Virginia. 91st Annu. Water Environ. Fed. Tech. Exhib. Conf. WEFTEC 2018 2018, 4298–4311. https://doi.org/10.2175/193864718825139005

McDonnell, B., Ratliff, K., Tryby, M., Wu, J., Mullapudi, A., 2020. PySWMM: The Python Interface to Stormwater Management Model (SWMM). J. Open Source Softw. 5, 2292. https://doi.org/10.21105/joss.02292

Meng, T., Hsu, D., Wadzuk, B., Asce, A.M., 2017. Green and Smart: Perspectives of City and Water Agency Officials in Pennsylvania toward Adopting New Infrastructure Technologies for Stormwater Management. J. Sustain. Water Built Environ. 3, 05017001. https://doi.org/10.1061/JSWBAY.0000824

Mohammadiun, S., Yazdi, J., Hager, J., Salehi Neyshabouri, S.A.A., Sadiq, R., Hewage, K., Alavi Gharahbagh, A., 2020. Effects of bottleneck blockage on the resilience of an urban stormwater drainage system. Hydrol. Sci. J. 65, 281–295. https://doi.org/10.1080/02626667.2019.1690657

Mugume, S., Gomez, D., Butler, D., 2014. Quantifying the Resilience of Urban Drainage Systems Using a Hydraulic Performance Assessment Approach, in: 13th International Conference on Urban Drainage. IAHR (International Association for Hydro-Environment) / IWA (International Water Association), Sarawak, Malaysia, pp. 7–12. https://doi.org/10.13140/2.1.3291.1047

Mugume, S.N., Gomez, D.E., Fu, G., Farmani, R., Butler, D., 2015. A global analysis approach for investigating structural resilience in urban drainage systems. Water Res. 81, 15–26. https://doi.org/10.1016/j.watres.2015.05.030

Mullapudi, A., Lewis, M.J., Gruden, C.L., Kerkez, B., 2020. Deep reinforcement learning for the real time control of stormwater systems. Adv. Water Resour. 140, 103600. https://doi.org/10.1016/j.advwatres.2020.103600

NOAA, 2010. National Weather Service [WWW Document]. Natl. Ocean. Atmos. Adm. URL https://www.weather.gov/abq/northamericanmonsoon-intro (accessed 7.11.20).

Ouyang, M., Dueñas-Osorio, L., Min, X., 2012. A three-stage resilience analysis framework for urban infrastructure systems. Struct. Saf. 36, 23–31. https://doi.org/10.1016/j.strusafe.2011.12.004

Panos, C.L., Wolfand, J.M., Hogue, T.S., 2021. Assessing resilience of a dual drainage urban system to redevelopment and climate change. J. Hydrol. 596, 126101. https://doi.org/10.1016/j.jhydrol.2021.126101

Park, J., Seager, T.P., Rao, P.S.C., Convertino, M., Linkov, I., 2013. Integrating risk and resilience approaches to

603 catastrophe management in engineering systems. Risk Anal. 33, 356–367. https://doi.org/10.1111/j.1539-
604 6924.2012.01885.x
605 Rathnayake, U., Faisal Anwar, A.H.M., 2019. Dynamic control of urban sewer systems to reduce combined sewer
606 overflows and their adverse impacts. J. Hydrol. 579, 124150. https://doi.org/10.1016/j.jhydrol.2019.124150
607 Rossman, L.A., Huber, W.C., 2016. Storm Water Management Model Reference Manual Volume I – Hydrology
608 (revised)(EPA/600/R-15/162A). U.S. Environ. Prot. Agency I, 231. https://doi.org/EPA/600/R-15/162 |
609 Sadler, J.M., Goodall, J.L., Behl, M., Bowes, B.D., Morsy, M.M., 2020. Exploring real-time control of stormwater
610 systems for mitigating flood risk due to sea level rise. J. Hydrol. 583, 124571.
611 https://doi.org/10.1016/j.jhydrol.2020.124571
612 Salerno, F., Viviano, G., Tartari, G., 2018. Urbanization and climate change impacts on surface water quality:
613 Enhancing the resilience by reducing impervious surfaces. Water Res. 144, 491–502.
614 https://doi.org/10.1016/j.watres.2018.07.058
615 Schmitt, Z.K., Hodges, C.C., Dymond, R.L., 2020. Simulation and assessment of long-term stormwater basin
616 performance under real-time control retrofits. Urban Water J. 17, 467–480.
617 https://doi.org/10.1080/1573062X.2020.1764062
618 Schütze, M., Campisano, A., Colas, H., Schilling, W., Vanrolleghem, P.A., 2004. Real time control of urban
619 wastewater systems - Where do we stand today? J. Hydrol. 299, 335–348.
620 https://doi.org/10.1016/j.jhydrol.2004.08.010
621 Sharior, S., McDonald, W., Parolari, A.J., 2019. Improved reliability of stormwater detention basin performance
622 through water quality data-informed real-time control. J. Hydrol. 573, 422–431.
623 https://doi.org/10.1016/j.jhydrol.2019.03.012
624 Shishegar, S., Duchesne, S., Pelletier, G., 2019. An integrated optimization and rule-based approach for predictive
625 real time control of urban stormwater management systems. J. Hydrol. 577, 124000.
626 https://doi.org/10.1016/j.jhydrol.2019.124000
627 SLCDPU, 2018. Storm Water and Flood Control [WWW Document]. URL https://www.slc.gov/utilities/stormwater-
628 and-flood-control/ (accessed 2.3.21).
629 Smith, K., Strong, C., Wang, S.Y., 2015. Connectivity between historical great basin precipitation and Pacific ocean
630 variability: A CMIP5 model evaluation. J. Clim. 28, 6096–6112. https://doi.org/10.1175/JCLI-D-14-00488.1

631 Tavakol-Davani, H., Burian, S.J., Devkota, J., Apul, D., 2016. Performance and Cost-Based Comparison of Green
632 and Gray Infrastructure to Control Combined Sewer Overflows. J. Sustain. Water Built Environ. 2, 04015009.
633 https://doi.org/10.1061/JSWBAY.0000805
634 Tavakol-Davani, H.E., Tavakol-Davani, H., Burian, S.J., McPherson, B.J., Barber, M.E., 2019. Green infrastructure
635 optimization to achieve pre-development conditions of a semiarid urban catchment. Environ. Sci. Water Res.
636 Technol. 5, 1157–1171. https://doi.org/10.1039/c8ew00789f
637 Teutschbein, C., Seibert, J., 2012. Bias correction of regional climate model simulations for hydrological climate-
638 change impact studies: Review and evaluation of different methods. J. Hydrol. 8, 12–29.
639 https://doi.org/10.1016/j.jhydrol.2012.05.052
640 Tousi, E.G., Brien, W.O., Doulabian, S., Toosi, A.S., 2021. Climate Changes Impact on Stormwater Infrastructure
641 Design in Tucson Arizona. Sustain. Cities Soc. 72, 103014. https://doi.org/10.1016/j.scs.2021.103014
642 Troutman, S.C., Love, N.G., Kerkez, B., 2020. Balancing water quality and flows in combined sewer systems using
643 real-time control. Environ. Sci. Water Res. Technol. 6, 1357–1369. https://doi.org/10.1039/c9ew00882a
644 United States Department of Agriculture, 2009. Design Rainfall Distributions Based on NOAA Atlas 14, USDA
645 NRCS Technical Paper.
646 Wang, S., Fu, J., Wang, H., 2019. Unified and rapid assessment of climate resilience of urban drainage system by
647 means of resilience profile graphs for synthetic and real (persistent) rains. Water Res. 162, 11–21.
648 https://doi.org/10.1016/j.watres.2019.06.050
649 Wang, Y., Meng, F., Liu, H., Zhang, C., Fu, G., 2019. Assessing catchment scale flood resilience of urban areas using
650 a grid cell based metric. Water Res. 163, 114852. https://doi.org/10.1016/j.watres.2019.114852
651 Wong, B.P., Kerkez, B., 2018. Real-Time Control of Urban Headwater Catchments Through Linear Feedback:
652 Performance, Analysis, and Site Selection. Water Resour. Res. 54, 7309–7330.
653 https://doi.org/10.1029/2018WR022657
654 Wright, D.B., Bosma, C.D., Lopez-Cantu, T., 2019. U.S. Hydrologic Design Standards Insufficient Due to Large
655 Increases in Frequency of Rainfall Extremes. Geophys. Res. Lett. 46, 8144–8153.
656 https://doi.org/10.1029/2019GL083235
657 Xu, W.D., Fletcher, T.D., Burns, M.J., Cherqui, F., 2020. Real Time Control of Rainwater Harvesting Systems: The
658 Benefits of Increasing Rainfall Forecast Window. Water Resour. Res. 56, 0–2.

https://doi.org/10.1029/2020WR027856

Zhang, D., Dong, X., Zeng, S., 2021. Exploring the structural factors of resilience in urban drainage systems: a large-scale stochastic computational experiment. Water Res. 188, 116475. https://doi.org/10.1016/j.watres.2020.116475